Formation of Range-Doppler Maps based on Sparse Reconstruction

Jabran Akhtar and Karl Erik Olsen

Norwegian Defence Research Establishment (FFI)
Box 25, 2027 Kjeller, Norway
Email: jabran.akhtar@ffi.no, karl-erik.olsen@ffi.no

***Abstract*— This paper presents an application of compressed sensing in a pulsed system such as a radar or sonar to form range-Doppler maps. Instead of transmitting a train of pulses we portrait a system where the pulse emission itself takes place in a sparse manner. We show that any empty data segments can effectively be filled in by sparse reconstruction which can also be used to extrapolate supplementary values. Simulations covering various conditions are used to demonstrate the effectiveness of the proposed setup.**

Keywords: Range-Doppler, Delay-Doppler, sparse reconstruction, coherent integration, target detection

I. Introduction

Pulsed sensing systems such as radars play a key role in surveillance, detection and tracking of targets. Such a system typically operates by transmitting a pulse and performing a matched filtering operation on the incoming delayed and Doppler-shifted pulse echoes. This process of transmitting and receiving incoming pulses is repeated a number of times (slow-time) within a defined coherent processing interval. The collected data is then often stacked together in a matrix and a Fourier transform across the slow-time domain is implemented to construct a range-Doppler map. A range-Doppler map can be used for target detection and tracking as it provides estimates of both range and velocity. Modern radars are further typically equipped with electronically steering arrays and are able to digitally steer a beam instantaneously. While emitting pulses at a specific direction a radar may desire to skip over a few pulses and rather transmit these towards a different angle for various purposes, such as tracking, and then come back to the main angle to resume standard operation. Alternatively, a radar may split the number of pulses available within a coherent processing interval between several directions and only transmit all the pulses at the same angle if some unusual activity does show up. This type of continuous beam switching, with the full array, introduces empty incoherent data gaps in the slow-time domain and a range-Doppler profile has to be composed with fewer pulses, resulting in limited integration gain and lower Doppler bin resolution. Lack of data within the dwell period may also occur due to other causes such as high duty cycle and hardware limitations.

In this regard, an open research topic is to what extent empty data segments can be reconstructed or interpolated from available data, particularly for the purpose of a range-Doppler map. In this work we propose the use of a compressed sensing (CS) framework [1], [2], [3] with emphasis on the slow-time / Doppler domain. Several previous papers have considered various aspects of employing CS and sparse reconstruction is a radar context [4], [5], [6], though the explicit construction of a range-Doppler map has not been given much attention. In contrast to for example [7], [6], [8], [9] we do not assume that the radar emits specific modulated subpulses or even a continuous pulse of trains in the same direction and also do not infer that the sampling is done in a sparse or irregular fashion. We presume that sampling of incoming echos at a given rate is not really a bottleneck issue and the presented concept instead emphasizes emission and thereupon reception of whole pulses in a sparse manner. Further on, we treat each range bin as a separate one-dimensional problem leading to the use of tractable partial Fourier matrices [10]. The motivation for CS and sparse reconstruction comes from the fact that a range-Doppler profile is likely to be sparse in nature. Each target typically occupies a few Doppler bins and as the overall contour is otherwise dominated by noise a sparse reconstruction strategy is likely to be competent at assembling a profile where the missing data has been repleted.

In addition to interpolating missing values, another important application of the method is to extrapolate data beyond the end points to formulate additional slow-time statistics. Extrapolating from a sparse reconstruction viewpoint, incorporating all available data, can be a promising extrapolating approach as the relationship between slow-time samples and Doppler domain is taken into account. It is noteworthy that before proceeding with a Fourier transform across slow-time, a windowing function is often applied to smooth out measurements and reduce sidelobe levels; data collected at the beginning and end of the assumed integration period is thus weighted down. An extrapolation can conjointly provide more substance in making maximum use of available data. An interesting example of extrapolation, though in a different context, has been presented in [11].

We show that the utilization of CS and sparse reconstruction has considerable merit for generating range-Doppler plots as empty slow-time segments can to a great extent be compensated and filled in. The same methods, through extrapolations, aid in improving the Doppler bin resolution and integration gain [12]. The concept is directly applicable to many types of

Dette er en postprint-versjon / This is a postprint version.
DOI til publisert versjon / DOI to published version: 10.1109/JSEN.2016.2577881

pulsing systems, such as sonars, though the remainder of the paper is radar centric.

II. Signal model

We consider a radar system where transmission and reception of N pulses takes place during a determined coherent interval. At each pulse repetition interval $p(t)$ is emitted and the incoming signal at slow-time u, $u = 1, 2, ..., N$, be described by

$$s(t,u) = \sum_n \sigma_n p(t-\Delta_n) e^{jv_{n,u}} + \tilde{w}(t) \tag{1}$$

where t is fast-time, σ_n are the reflectivity levels of incoming echoes and targets while Δ_n is the signal delay associated with each reflector and $j = \sqrt{-1}$. $\tilde{w}(t)$ is white Gaussian noise, $e^{jv_{n,u}}$ is the experienced Doppler phase shift which for a constant velocity object is typically modeled by

$$v_{n,u} = v_{n,u-1} + \frac{r_n \, 4\pi f_c}{c \, \text{PRF}}, \tag{2}$$

where r_n is the radial velocity of target n, f_c being the carrier frequency, PRF is the pulse repetition frequency and c is the speed of light [13]. For convenience we can define $v_{n,0} = 0$. It is assumed that within the coherent time frame of N pulses the targets do not undergo any significant alteration in amplitude and there is no noticeable shift in time delay.

After transmission of each waveform the radar samples any incoming pulse reflections and a matched filtering operation is carried out via the time-reversed and conjugated pulse $p^*(-t)$. The pulse compressed data can then be specified as

$$Y(t,u) = p^*(-t) * s(t,u) = \sum_n \sigma_n \text{psf}_p(t-\Delta_n) e^{jv_{n,u}} + w(t) \tag{3}$$

where $*$ prescribes convolution in fast-time and $\text{psf}_p(t) = p(t) * p^*(-t)$ is the pulse spreading function. In a practical setting the fast-time parameter will also be discrete, we denote this explicitly as

$$\mathbf{Y}(t_m, u) = Y(t_m \Delta t, u) \ \in \mathbb{C}^{N \times R}, \ t_m = 1, 2, ..., R, \tag{4}$$

given Δt as the time-resolution of the radar. $R\Delta t$ thus corresponds to the largest time-delay associated with the maximum unambiguous radar range.

For further processing $\mathbf{Y}(t_m, u)$ is typically multiplied in slow-time by a windowing function $\mathbf{w}(u) \ \in \mathbb{C}^{N \times 1}$ to yield

$$\mathbf{Y}_W(t_m, u) = \mathbf{w}(u)\mathbf{Y}(t_m, u) \ \in \mathbb{C}^{N \times R}. \tag{5}$$

Performing a Fourier transformation with respect to slow-time, over all discrete time-delays, or equivalently ranges, results in the range-Doppler map matrix $\mathbf{D}$:

$$\mathbf{D}(t_m, \omega) = \mathbf{F} \ \mathbf{Y}_W(t_m, u) \ \in \mathbb{C}^{N \times R}. \tag{6}$$

$\mathbf{F}$ is the discrete Fourier matrix of size $N \times N$, $\mathbf{F}_{k,l} = \exp(2\pi jkl/N)$. Notice that the above process is independent for each range bin and can also be executed through an FFT to make it computationally more efficient. ω can readily be converted into $[-v_{max} \ \ v_{max}]$ where $v_{max} = \frac{c \, \text{PRF}}{4 f_c}$ is the maximum unambiguous velocity [13], with the resolution in Doppler bin space determined by N, $\Delta\omega = \frac{2\pi}{N}$. The Doppler bin resolution hence refers to the number of bins in the velocity domain which is directly related to the number of measurements in slow-time. In the Doppler profile the main factors forming the contour will be phase shifts originating from (2). Targets showing a consistent velocity within the dwell period will after Fourier processing appear concentrated in Doppler; only occupying a few select velocity bins subject to noise, measurement inaccuracies and the applied window function. As long as there are only a few targets at each range bin this leads to an overall sparse profile.

A. Sparse reconstruction

We assume that for whatever reason the radar does not transmit N pulses right after each other in the same direction rather the truncated $\tilde{\mathbf{Y}}(t_m, \tilde{u}) \in \mathbb{C}^{K \times R}$ only contains $K < N$ slow-time measurements, $\tilde{u} = 1, 2, ..., K$, collected arbitrary within the coherent interval of N pulses. The slow-time positions where data is collected is designated by the set D. With a curtailed dataset the measured Doppler model will follow a discontinuous form

$$v_{n,\tilde{u}} = v_{n,\tilde{u}-1} + k(\tilde{u}) \frac{r_n \, 4\pi f_c}{c \, \text{PRF}}. \tag{7}$$

The discrepancies associated with the transmission pattern are provided by the function $k(\tilde{u}) \in \mathbb{N}$ and a $k(\hat{u})|_{\hat{u}=v} > 1$ indicates a phase jump due to irregular sampling in slow-time. A typical range-Doppler plot may now still be constructed by applying a Fourier matrix of size $K \times K$ on each range bin, however, with incoherent data this will result in spectral leakage and lower integration gain.

The method we introduce is to assemble an extended range-Doppler profile using a sparse reconstruction procedure and thus attempt to retain a high resolution in slow-time. This can be accomplished if from the K slow-time measurements we can interpolate and fill in the missing $N - K$ values thus bringing the number of bins back to N. The objective being to preserve the Doppler bin resolution and potentially also the accuracy even though fewer pulses have actually been emit. This will also transform incoherent measurements into a coherent form suitable for a range-Doppler plot without spectral leakage. The process can likewise be extended to extrapolate additional bins on the edges. This will further increment the Doppler bin resolution and with a satisfactory extrapolation of targets provide a narrower velocity response.

The ideal solution should inter- and / or extrapolate to expand (7) into a form of (2) with constant phases across slow-time as only this would lead to full focusing of each individual target in Doppler. Consequently, as the overall profile is assumed to be sparse in Doppler the solution will be the one that maximizes sparsity in this domain. For this we define L to indicate the number of desired output entries in slow-time and assume that $L \geq N$; an $L > N$ signifying extrapolation. The reconstructed profile in slow-time is denoted by $\hat{\mathbf{Y}}(t_m, \hat{u}) \in \mathbb{C}^{L \times R}$, $\hat{u} = 1, ..., L$ and the relationship to range-Doppler map

Dette er en postprint-versjon / This is a postprint version.
DOI til publisert versjon / DOI to published version: 10.1109/JSEN.2016.2577881

is as previously governed by

$$\hat{\mathbf{D}}(t_m, \hat{\omega}) = \hat{\mathbf{F}}\ \hat{\mathbf{w}}(\hat{u})\hat{\mathbf{Y}}(t_m, \hat{u})\ \in \mathbb{C}^{L\times R} \tag{8}$$

where $\hat{\mathbf{F}}$ is an $L \times L$ Fourier matrix. We further define a binary selection matrix $\mathbf{M} \in \mathbb{B}^{K\times L}$ by taking an $L\times L$ identity matrix $\mathbf{I}_{L\times L}$ and removing respective rows for which no collected data is available. We specify this as

$$\mathbf{M} = H_D(\mathbf{I}_{L\times L}) \tag{9}$$

where the function H_D only preserves the rows of the given matrix as specified by the set D. This purpose of the selection matrix is to allow for extraction of values from positions where slow-time data has been accumulated. We further form $\bar{\mathbf{w}}(\tilde{u})$ by selecting a windowing function of L entries, $\hat{\mathbf{w}}(\hat{u}) \in \mathbb{C}^{L\times 1}$, and truncating it to K values:

$$\bar{\mathbf{w}}(\tilde{u}) = \mathbf{M}\hat{\mathbf{w}}(\hat{u})\ \in \mathbb{C}^{K\times 1} \tag{10}$$

The reconstructed matrix should have the same set of values at measured data placements, which can be expressed as

$$(\mathbf{M}\hat{\mathbf{Y}})(t_m, \tilde{u}) = \tilde{\mathbf{Y}}(t_m, \tilde{u}), \tag{11}$$

for notational simplicity the index terms are only given for the final product. With windowing functions incorporated the requirement becomes

$$\mathbf{M}(\hat{\mathbf{w}}\hat{\mathbf{Y}})\ (t_m, \tilde{u}) = (\mathbf{M}\hat{\mathbf{w}})\tilde{\mathbf{Y}}\ (t_m, \tilde{u}). \tag{12}$$

We can re-write this as

$$(\mathbf{M}\hat{\mathbf{F}}^*\hat{\mathbf{F}}\hat{\mathbf{w}}\hat{\mathbf{Y}})\ (t_m, \tilde{u}) = \bar{\mathbf{w}}\tilde{\mathbf{Y}}\ (t_m, \tilde{u}) \tag{13}$$

which leads to

$$\hat{\mathbf{F}}_R\hat{\mathbf{D}}\ (t_m, \hat{\omega}) = \bar{\mathbf{w}}\tilde{\mathbf{Y}}\ (t_m, \tilde{u}), \tag{14}$$

given the partial inverse Fourier matrix $\hat{\mathbf{F}}_R = \mathbf{M}\hat{\mathbf{F}}^*\ \in \mathbb{C}^{K\times L}$.

As the reconstructed solution is assumed to be sparse in Doppler it is most approachable to recover it directly in this domain. Given a particular range $T = t_m$ the objective is therefore to determine a sparse Doppler profile $\hat{\mathbf{D}}(T, \hat{\omega})$ consisting of L Doppler samples while assenting with the observations. The reconstruction problem under convex relaxation can accordingly be formulated as

$$\hat{\mathbf{D}}(T, \hat{\omega}) = \arg\min ||\dot{\mathbf{D}}(T, \hat{\omega})||_1 \tag{15}$$

subject to the constraint

$$||\ \hat{\mathbf{F}}_R\ \dot{\mathbf{D}}(T, \hat{\omega}) - \bar{\mathbf{w}}(\tilde{u})\ \tilde{\mathbf{Y}}(T, \tilde{u})\ ||_2 \leq \varepsilon \tag{16}$$

where ε is acceptable error limit. The constriction is a relaxed version of (14) in order to accommodate for the presence of noise and other inaccuracies. Finding an independent solution over all defined values of $t_m = 1, 2, ..., R$ results in range-Doppler map matrix $\hat{\mathbf{D}}(t_m, \hat{\omega})$ where any missing data would effectively have been inter- or extrapolated. As this process is independent for each range-bin it may be executed in parallel. Several efficient algorithms have been proposed in the literature with regard to sparse reconstruction [2], [13], [14], [15] and we refer to them for more details. The bin resolution of $\hat{\omega}$ in (14) and (15) is now conditioned by L, $\Delta\hat{\omega} = \frac{2\pi}{L}$.

The inverse Fourier matrix $\hat{\mathbf{F}}_R$ has a crucial role in CS algorithms in order to find a unique and exact solution to the posed problem. Fortunately, partial Fourier matrices have been well studied in the literature as they are often encountered in various scenarios and have been shown to provide competent performance in CS problems [1], [10], [16]. The design of the transmission pattern defined by the set D which results in $\hat{\mathbf{F}}_R$ can be selected randomly (e.g. random beam switching) [1], [17] or designed deterministically (e.g. predetermined beam switching pattern) where the matrix can be optimized beforehand [14], [18], [19]. An important aspect with regard to perfect recovery is related to the minimum number of required measurements. For that, it has been shown in e.g. [17] that for random Fourier, and similar, matrices the number of measurements needs to be on the order of $K = O(s_T \log^4 L)$ for a perfect recovery, where s_T corresponds to the number of targets of the Doppler profile $\mathbf{D}(T, \omega)$. Nevertheless, these bound contain several unsettled scaling factors which makes it difficult to determine how many measurements, or in our case pulse emission and receptions, are really required to form a range-Doppler map of sufficient quality.

Increasing L by adding extrapolating points at the beginning and end of the sequence forces an increment on the resolution of the Doppler profile by appending additional bins. A solution to the problem as posed here must still attempt to maximize the sparsity which is achieved if objects of interest are extrapolated with a determined velocity and consequently gets confined more and more narrowly to an exact velocity.

In order to evaluate the practicability of sparse reconstruction and demonstrate the principles introduced we therefore resort to simulations in the next section to quantify the performance for standard sparse scenes as normally experienced by e.g. long range sensing radars.

III. Simulated scenarios

This section reviews the performance of CS and seeks restoration of range-Doppler maps with limited amount of available data. For this end we employ an in-house radar simulator which can simulate various conditions. Two Swerling 1 targets with radar cross section of $0.1m^2$ (T1) and $0.3m^2$ (T2) are simulated with velocities of -20m/s and 20m/s. Targets altitude is 10m and are placed, respectively, approximately 92 and 125km from the sensor. Although both targets have a low radar cross section having a two target scenario allows us to track for any arising discrepancies and it is also possible to view T1 as a version of T2 where due to e.g. range walk or other issues the target appears much dimmer. The coherent period is assumed to correspond to $N = 32$ pulses. The radar propagation path is modeled with APM [20] and antenna parameters follow beamwidths of 2°, altitude 1000m operating at 3GHz, a bandwidth of 0.8 MHz, emitting power at 15kwatt, antenna transmit and receive gain of 37dB and an PRF of 3000. The average noise figure evaluates to -103dBm and the Blackman window has been utilized throughout. The sparse

Dette er en postprint-versjon / This is a postprint version.
DOI til publisert versjon / DOI to published version: 10.1109/JSEN.2016.2577881

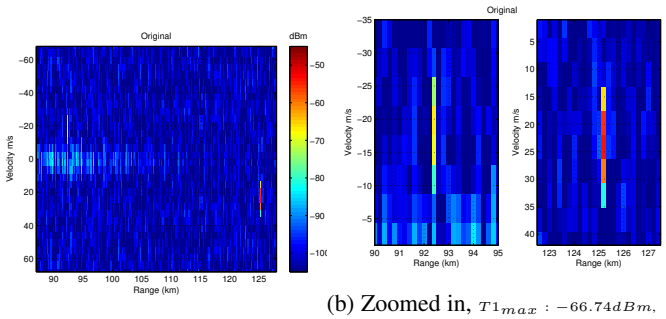

(a) Full

(b) Zoomed in, $T1_{max}: -66.74dBm$, $T2_{max}: -53.76dBm$

Fig. 1: Original R-D map with 32 pulses

solutions are found through a spectral projection gradient method [15] and ε is computed by estimating the average noise level and scaling it by L. The displayed results are found after a single run of the algorithm for each range-bin.

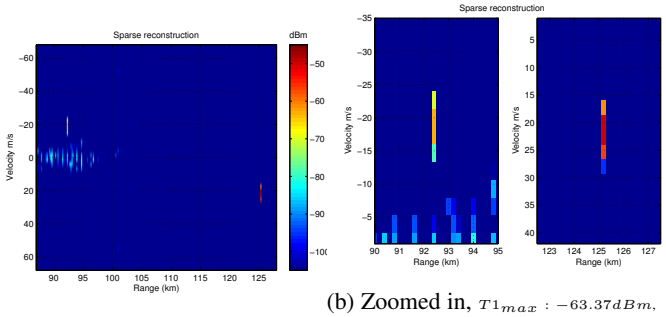

(a) Full

(b) Zoomed in, $T1_{max}: -63.37dBm$, $T2_{max}: -50.05dBm$

Fig. 2: Sparse reconstruction, 10 extrapolations on both ends

A. *Extrapolation only*

We first consider an example case where the radar transmits $N = 32$ pulses in the same direction with no deviation and sparse reconstruction with (15) and (16) is solely used to extrapolate ten additional values at both ends. This leads to $L = 52$ samples in slow-time with a correspondingly forced increase in Doppler bin resolution.

Figure 1 shows the original $N = 32$ pulse standard range-Doppler plot generated from simulated data with a Fourier transform and the objects span around 4 Doppler bins of prominent value. All range-Doppler maps shown display the results from the full $||\mathbf{D}(t_m, \omega)||^2$, the truncated $||\tilde{\mathbf{D}}(t_m, \tilde{\omega})||^2$ or the reconstructed $||\hat{\mathbf{D}}(t_m, \hat{\omega})||^2$ with logarithmic scaling between -105dBm to -45dBm. In the original case the SNR, after processing, amounts to 35.71dB for T1 and 48.51dB for T2. The outcome from extrapolated sparse reconstruction with a total of 20 extra Doppler bins is given in figure 2 where the targets are still retained within the same number of bins but now overall resulting in a narrower response greatly improving the velocity accuracy. In addition, there is an increase in the peak energy level for both targets of around 3dB. Notice that a sparse solution will contain a large number of values identical to zero making it impractical to compute the signal to noise ratios.

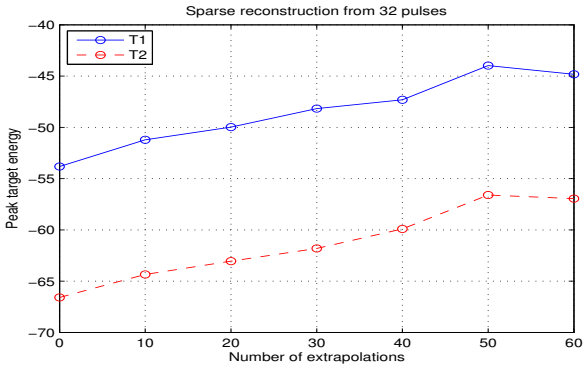

Fig. 3: Peak target power

In order to quantify the impact of varying number of extrapolations, figure 3 displays the average peak target values for both target T1 and T2 over 1000 simulations as the number of extrapolations, split equally on both sides, is varied from 0 to 60 under randomly generated noise. The integration gain keeps building while simultaneously the velocity estimates are narrowed down. This though also occurs for e.g. any clutter, see figure 4 for examples of extracted Doppler profiles, at target ranges, generated with various number of extrapolations under sparse reconstruction. The main purpose of this is to show that the extrapolation process is indeed taking place correctly with respect to the given target. One should be mindful of this increase in energy if a conversion back to slow-time is performed.

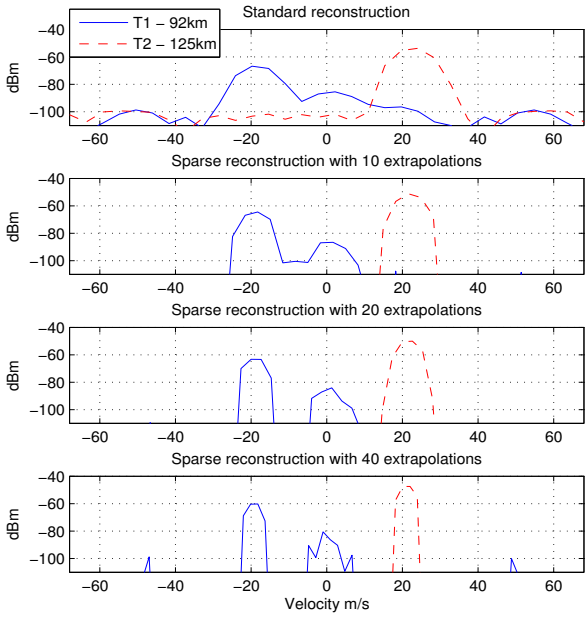

Fig. 4: Doppler profiles for varying number of extrapolations

For classic sparse radar scenes extrapolation through sparse

Dette er en postprint-versjon / This is a postprint version.
DOI til publisert versjon / DOI to published version: 10.1109/JSEN.2016.2577881

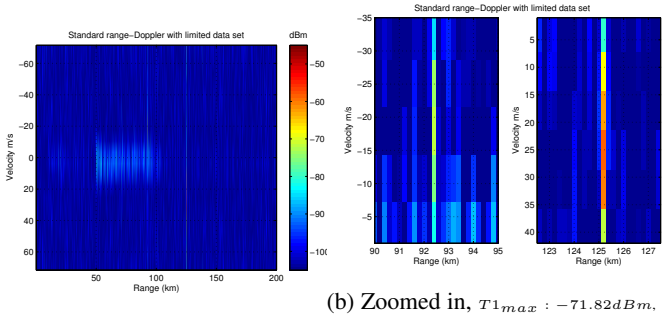

(a) Full

(b) Zoomed in, $T1_{max}: -71.82dBm$, $T2_{max}: -59.04dBm$

Fig. 5: Standard R-D map with 20 random pulses (out of 32)

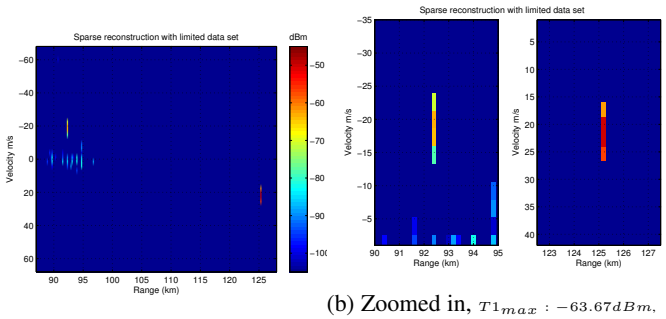

(a) Full

(b) Zoomed in, $T1_{max}: -63.67dBm$, $T2_{max}: -50.13dBm$

Fig. 6: Sparse reconstruction with 20 random pulses (out of 32) and 20 extrapolations

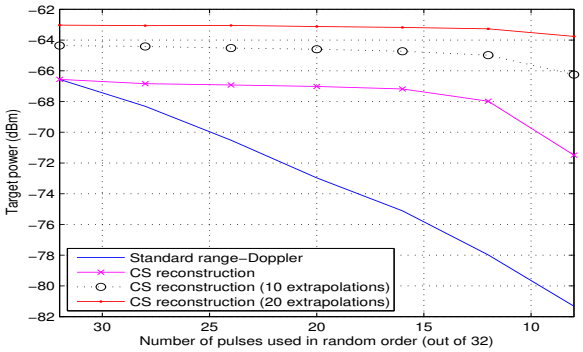

Fig. 7: Averaged peak target energy T1

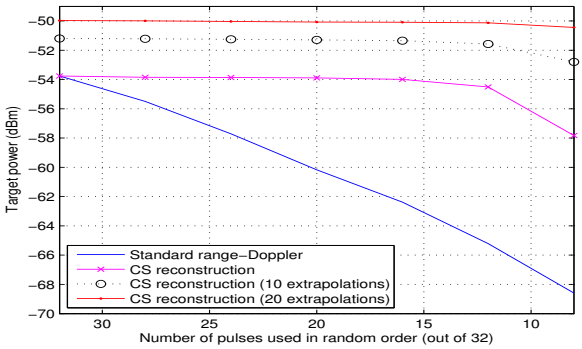

Fig. 8: Averaged peak target energy T2

reconstruction can augment radar performance in a noticeable manner.

B. Random beam switching

A more typical implementation of the CS emission and reception strategy is to have consecutive exchanging beams in the same coherent time frame where the radar transmits pulses randomly at selected angles. The sparse reconstruction scheme can then be used to fill in empty positions and extrapolate in the same procedure to maintain a high comparative resolution in Doppler as if all pulses had been emitted in the same direction.

An example of this is demonstrated next where the radar only transmits $K = 20$ pulses, out of standard $N = 32$, in a random order, at the main direction. Figure 5 shows the outcomes in the case of standard pulse-Doppler processing with degraded Doppler bin resolution and accuracy due to limited slow-time data. Both targets are likewise dimmer with spectral leakage. The result from sparse reconstruction incorporating 20 extrapolations ($L = 52$), with the identical data, given in figure 6 is very contrasting. The targets stand out clear with a comparable power level and still preserving good accuracy in Doppler much in line with figure 2.

Figures 7 and 8 show more comprehensive graphs over how the average peak target energy varies with varying number of available pulses and sparse reconstruction with or without extrapolation alongside standard range-Doppler processing. The averaging is carried over 1000 randomly different transmission patterns. An averaging is here carried out to help evaluate the performance under various transmission patterns rather than one specific emission structure. While there is a subtle decrease as the number of pulses is reduced the plots do manifest that a sparse reconstruction is able to retain the target power level well beyond and the extrapolation gain is preserved to a high degree.

With very limited amount of pulses available, the target peak power is still maintained, however, the Doppler profile start showing structural breakup and ghost targets. For a visual demonstration of this deterioration figure 9 details some examples of reproduced Doppler profiles for targets T1 and T2 with various number of randomly available pulses and assuming 10 extrapolations on both sides.

An important measure for accurate reconstruction is therefore the target span diversification accounting for number of bins occupied by a target. Figure 10 depicts the average number of Doppler bins, for the specific target ranges, who exceed the noise threshold by 20dB under different number of available pulses. Both standard Fourier transform and sparse reconstruction is compared and averaged over 1000 runs. A spread across too many bins reveals inaccurate estimation and spectral leakage whereas too few bins imply a more dim object or tight signal reconstruction. As T1 is a low reflecting target the number of Doppler bins occupied by it declines more rapidly as fewer and fewer pulses are available for reassembly. Nevertheless, sparse reconstruction with extrapolations is able

Dette er en postprint-versjon / This is a postprint version.
DOI til publisert versjon / DOI to published version: 10.1109/JSEN.2016.2577881

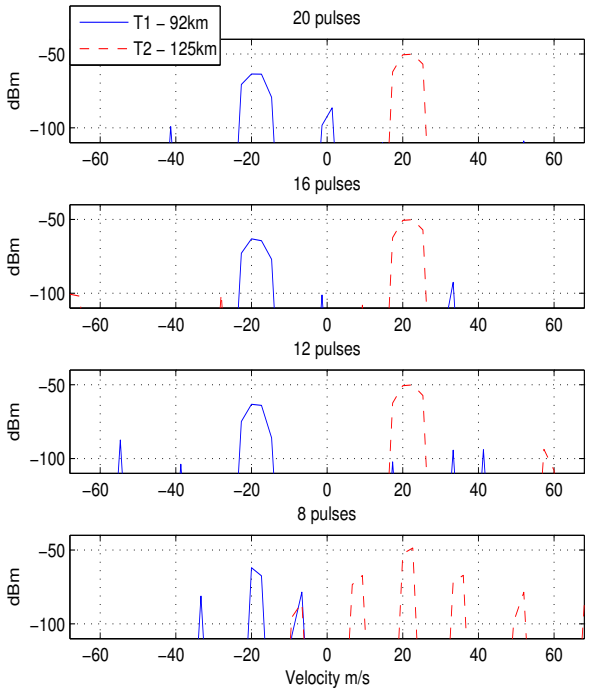

Fig. 9: Examples of sparse reconstructed Doppler profiles for varying number of available pulses

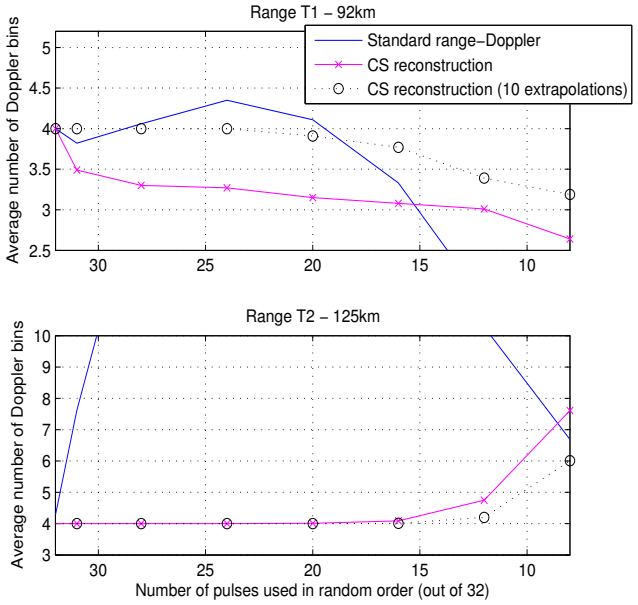

Fig. 10: Average number of Doppler bins exceeding threshold

to preserve the spread to approximately four bins as long as at least $K \geq 20$ pulses are available. For T2 (lower plot) the average number of Doppler bins remains at four bins if $K \geq 15$ is fulfilled, otherwise the target is no longer as firmly focused. This further lends support to the effectiveness of the sparse restoration approach as long as extreme low data circumstances are avoided.

In contrast, reconstruction with basic Fourier transform delivers much more fluctuating results, even with the lack of just a few pulses, due to uncontained spectral leakages and with low energy as shown in the previous plots.

The focus of this work has been on sparse surroundings, however, sparse reconstruction may well be utilized in the presence of multiple targets in the same Doppler bin. With less sparsity, the number of pulses required for CS to yield acceptable results will though increase; we do note that if the number of pulses is insufficient to resolve a target then the target gets spread out over several potential velocities (see e.g. figure 9) which in itself starts to reveal inaccurate reconstruction. The radar can then emit more pulses at the specific direction or alter the processing interval. A study on these aspects will be presented in future work.

IV. Conclusion

Range-Doppler maps are of great importance in modern radar systems and this work proposed application of sparse reconstruction techniques for their formation. It was shown that a radar may reduce the number of pulses transmitted in a coherent processing interval and effectively regenerate missing data. Simulations were used to demonstrate that good quality maps can be obtained with moderate amount of radar data under typical sparse conditions. The same approach can also be extended to extrapolate additional values at the beginning and end of a sequence to increase Doppler bin resolution.

References

[1] E. Candès, J. Romberg, and T. Tao, "Stable signal receovery from incomplete and inaccurate measurments," *Communication in Pure and Applied Mathematics*, vol. 59, pp. 1207–1223, 2006.

[2] L. C. Potter, E. Ertin, J. T. Parker, and M. Cetin, "Sparsity and compressed sensing in radar imaging," *Proceedings of the IEEE*, vol. 98, no. 6, pp. 1006–1020, 2010.

[3] M. F. Durate and Y. C. Eldar, "Structured compressed sensing: From theory to applications," *IEEE Transactions on Signal Processing*, vol. 59, pp. 4053–4085, 2011.

[4] M. Amin, F. Ahmad, and Z. Wenji, "A compressive sensing approach to moving target indication for urban sensing," in *IEEE Radar Conference*, 2011, pp. 509–511.

[5] R. A. Sevimli, M. Tofighi, and A. E. Cetin, "Range-doppler radar target detection using denoising within the compressive sensing framework," in *European Signal Processing Conference*, 2014, pp. 1950–1954.

[6] B. Pollock and N. A. Goodman, "Detection performance of compressively sampled radar signals," in *IEEE Radar Conference*, 2011, pp. 1117–1122.

[7] M. A. Herman and T. Strohmer, "High-resolution radar via compressed sensing," *IEEE Trans. Signal Processing*, vol. 57, no. 6, pp. 2275–2284, June 2009.

[8] T. Xing, W. Roberts, L. Jian, and P. Stoica, "Range-doppler imaging via a train of probing pulses," *IEEE Trans. Signal Processing*, vol. 57, no. 3, pp. 1084–1097, March 2009.

[9] M. M. Hyder and K. Mahata, "Range-doppler imaging via sparse representation," in *IEEE Radar Conference*, 2011, pp. 486–491.

[10] D. L. Donoho and J. Tanner, "Observed universality of phase transitions in high-dimensional geometry, with implications for modern data analysis and signal processing," *Philosophical Transactions of the Royal Society A: Mathematical, Physical and Engineering Sciences*, vol. 367, no. 1906, pp. 4273–4293, Nov. 2009.

Dette er en postprint-versjon / This is a postprint version.
DOI til publisert versjon / DOI to published version: 10.1109/JSEN.2016.2577881

[11] L. Anitori, W. van Rossum, and A. Huizing, "Array aperture extrapolation using sparse reconstruction," in *IEEE Radar Conference*, 2015, pp. 237–242.
[12] E. J. Candès and C. Fernandez-Granda, "Towards a mathematical theory of super-resolution," *Communications on Pure and Applied Mathematics*, vol. 67, no. 6, pp. 906–956, 2014.
[13] W. L. Melvin and J. A. S. (Eds.), *Principles of Modern Radar*. SciTech Publishing, 2013.
[14] M. Fornasier and H. Rauhut, *"Compressive sensing" in "Handbook of mathematical methods in imaging" O. Scherzer (Eds.)*. Springer New York, 2011.
[15] E. van den Berg and M. P. Friedlander, "Probing the pareto frontier for basis pursuit solutions," *SIAM Journal on Scientific Computing*, vol. 31, no. 2, pp. 890–912, 2008.
[16] B. Adcock, A. C. Hansen, C. Poon, and B. Roman, "Breaking the coherence barrier: asymptotic incoherence and asymptotic sparsity in compressed sensing," in *International Conference on Sampling Theory and Applications*, July 2013.
[17] M. Rudelson and R. Vershynin, "Sparse reconstruction by convex relaxation: Fourier and gaussian measurements," in *Annual Conference on Information Sciences and Systems (CISS)*, 2007, pp. 207–212.
[18] N. Y. Yu and Y. Li, "Deterministic construction of Fourier-based compressed sensing matrices using an almost difference set," *EURASIP Journal on Advances in Signal Processing*, vol. 155, pp. 805–821, Oct. 2013.
[19] G. Xu and Z. Xu, "Compressed sensing matrices from Fourier matrices," *IEEE Trans. Inf. Theory*, vol. 61, no. 1, pp. 469–478, Jan. 2015.
[20] A. E. Barrios, "Considerations in the development of the advanced propagation model (APM) for U.S. Navy applications," in *IEEE Radar Conference*, 2003, pp. 77–82.